Electronic Supplementary Material (ESI) for Journal of Materials Chemistry C.
This journal is © The Royal Society of Chemistry 2020

Two-stage metal ion sensing through space and through bond charge transfer

Guoxin Yin,[†a] *Yu Wang,*[†a] *Yuping Yuan,*[†a,c] *Ruxue Li,*[b] *Rui Chen,*[b] *Hsing-Lin Wang,*[*a]

[a]Department of Materials Science and Engineering
Southern University of Science and Technology
1088 Xueyuan Avenue, Shenzhen, 518055, P.R. China

[b]Department of Electrical and Electronic Engineering
Southern University of Science and Technology
1088 Xueyuan Avenue, Shenzhen, 518055, P.R. China

[c]Academy for Advanced Interdisciplinary Studies
Southern University of Science and Technology
1088 Xueyuan Avenue, Shenzhen, 518055, P.R. China

[†]These authors contributed equally to this work

Contents

1. Experimental Section

1.1 Reagents and Materials. All the reagents were obtained from commercial suppliers and were utilized without further purification. Tetrahydrofuran, acetonitrile and all the chloride salts of metal ions were purchased from Aldrich. All the other reagents used in the experiments were of spectroscopic grades.

1.2 Measurements of UV and PL. Fluorescence emission spectra were recorded using HORIBA PTI-QM-8075 Luminescence spectrometer. UV absorption spectra were performed on Cary 5000 UV-vis-NIR spectrophotometer. A quartz cuvette with 1 cm width and 3.5 cm height was used. Ligand BPVMB stock solutions, 1 mM, were prepared in acetonitrile (ACN). The metal ion (Na$^+$, Mg^{2+}, Ca^{2+}, Pb^{2+}, Cd^{2+}, Mn^{2+}, Ni^{2+}, Cu^{2+}, Zn^{2+} and Fe^{3+}) stock solutions were prepared in ACN in the order of 4 mM. All working solutions were prepared by gradual dilution of the stock solutions. The excitations wavelength was 320nm for ligand BPVMB with 3nm emission and excitation slit widths.

1.3 Measurements of Femtosecond Transient Absorption (TA) Spectrum. The TA spectra and dynamics were obtained using a standard pump−probe configuration at 350 nm, ∼100 fs pump pulses at a 1 kHz repetition rate, and a broad-band white-light supercontinuum probe (18SI80466 Rev.1, Newport). The excited power was 4 mW and the spot diameter was 300 μm.

2. Supplementary Methods

2.2 Determination of Apparent Dissociation Constant Fluorescence spectroscopy was used to determine the apparent dissociation constants (*K_d*) of 1 (50 μM) with Zn^{2+} and Cd^{2+}, using the reported method.[1] The fluorescence intensity data were fitted to equation 1, and K_d was calculated:

$$F = F_0 + (F_{max} - F_0)\frac{[M^{3+}]_{free}}{K_d + [M^{3+}]_{free}}$$

(1)

where F is the fluorescence intensity, F_{max} is the maximum fluorescence intensity, F_0 is the fluorescence intensity with no addition of Fe^{3+} and Cu^{2+}, and $[M^{3+}]_{free}$ is the free Fe^{3+} and Cu^{2+} concentration.

2.3 Synthesis of BPVMB. 1,3-diiodo-2-methoxybenzne (500mg, 1.39mmol) and 4-vinylpyridine (0.3ml, 2.78mmol) were dissolved in the 10ml N,N-dimethylformamide and 10ml diisopropylethylamine in a flask. The mixture was bubbled with N_2 for 20min and palladium acetate (15.7mg, 0.07mmol) and tris(2-methylphenyl)phosphine (30.4mg, 0.1mmol) were added into the mixture under N_2 flow. The reaction was stirred at 100°C under N_2 for 24h. The reaction was cooled to room temperature and filtered through celite. The filtrate was collected and evaporated in vacuum. The crude product was purified by column chromatography with methanol/ethyl acetate (1/4, volume ratio) as eluent. After removing the solvent, 340.5mg white crystal was collected with yield of 78%. ^{1}H-NMR (400MHz, $CDCl_3$), δ 8.59 (d, 4H, *J*=8Hz), 7.63(d, 2H, *J*=4Hz), 7.61(d, 2H, *J*=4Hz), 7.40(d, 4H, *J*=8Hz), 7.20(t, 1H, *J*=8Hz), 7.07(d, 2H, *J*=16Hz), 3.81(s, 3H); ^{13}C-NMR (100MHz, $CDCl_3$), δ 156.65, 150.29, 144.71, 130.37, 123.73, 127.32, 127.11, 124.84, 120.98, 62.61

3. Supporting Figures

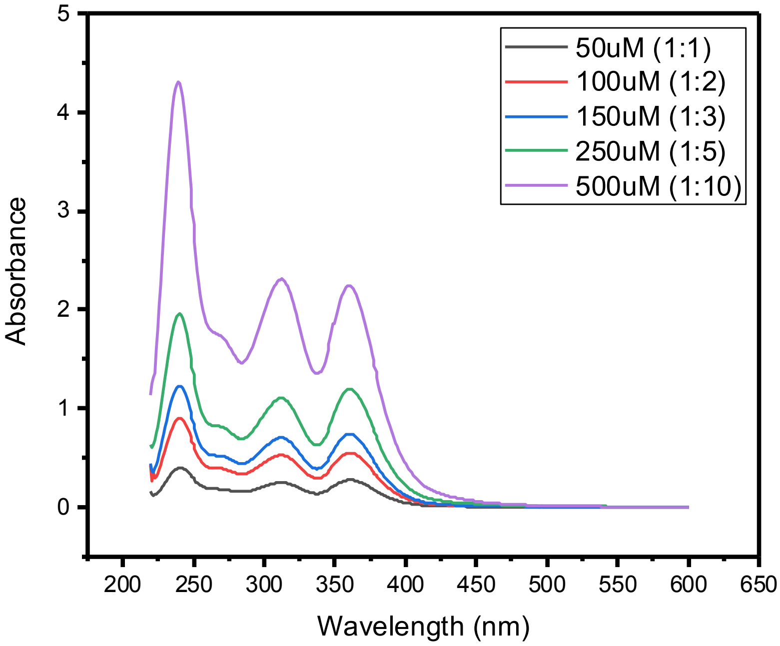

Fig. S1 Absorption spectra of Fe^{3+} in ACN at the concentration of 50 μM, 100 μM, 150 μM, 250 μM and 500 μM, respectively. The absorption spectrum exhibits λ_{max} at 240nm, 320nm, 360nm for Fe^{3+} in ACN with concentration between 50 μM and 500 μM.

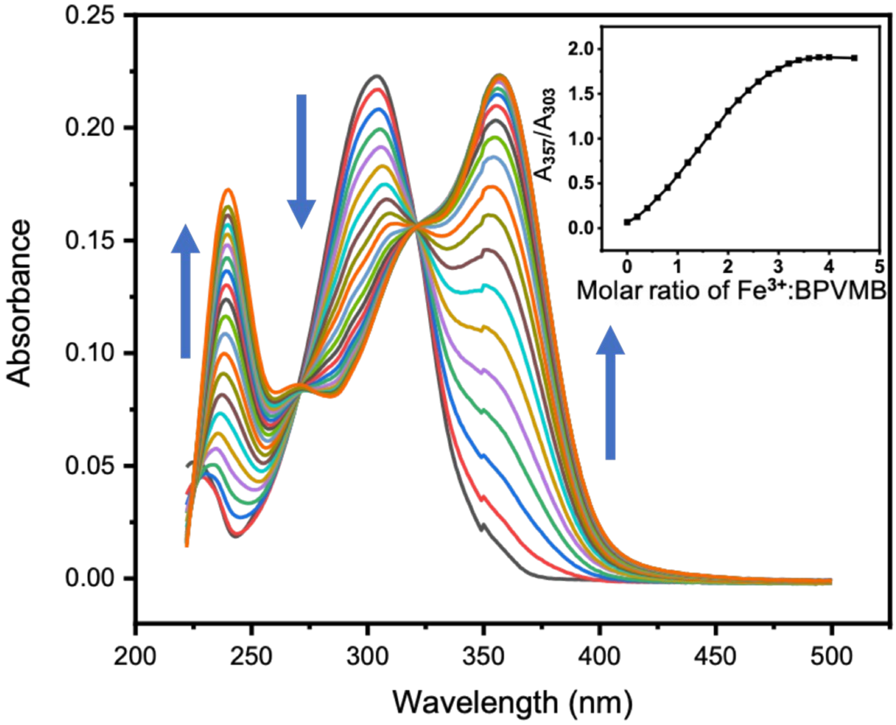

Fig. S2 Absorption spectra of BPVMB (5 μM) in ACN obtained by adding aliquots of 112.5 μL $FeCl_3$ (0.4 mM) solution. The [Fe^{3+}] total increases from 0.0 to 22.5 μM along the direction of the arrow. Inset, the titration profile based on the absorbance ratio at 357 and 303 nm, A_{357}/A_{303}. Upon addition of Fe^{3+} to the BPVMB solution, the peak at ~300 nm gradually red-shifts and eventually disappears with a concomitant increase of two new peaks at 240nm and 360nm. These two peaks are due to the increasing concentration of Fe^{3+}. The isosbestic points at 275nm and 325nm indicate that the spectra change is due to relative compositional changes between BPVMB and Fe^{3+}.

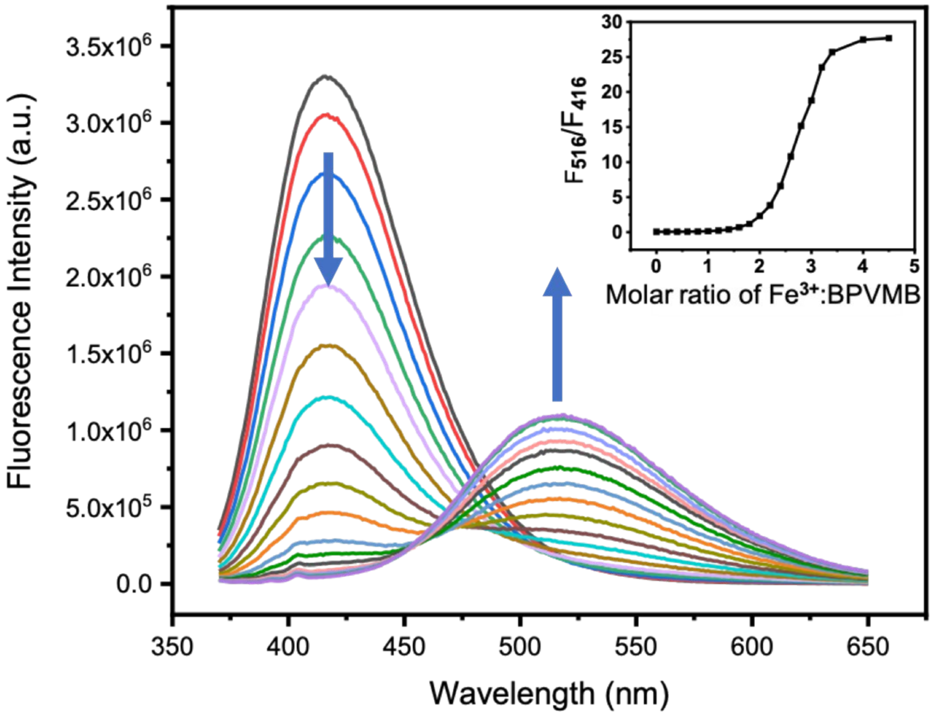

Fig. S3 Emission spectra of BPVMB (5 μM) in ACN obtained by adding aliquots of 112.5 μL $FeCl_3$ (0.4 mM) solution. Inset, the titration profile based on the emission ratio at 516 and 416 nm, F_{516}/F_{416}. Excitation was at 350 nm. As the addition of Fe^{3+} to the receptor solution, a red-shifted broad emission band centered at 530nm, which is highly likely due to the BPVMB-Fe^{3+} complex formation through bonding of the pyridine nitrogen with Fe^{3+}.

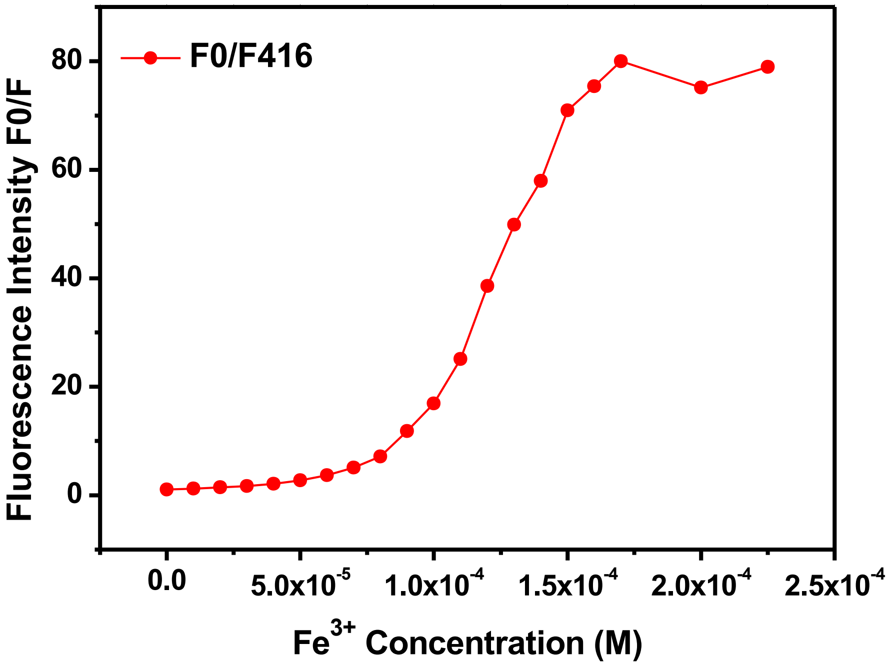

Fig. S4 Stern–Volmer plot of the quenching of the luminescence of nanoparticles of BPVMB by Fe^{3+} at λ_{em}=416nm (blue). The upward curvature of Stern-volmer plot is typical for situations in which both dynamic quenching and static quenching occur.[2] Such type of plot indicates a complex interaction mechanism, which suggests the presence of specific binding interactions, connected with more than one form of fluorophore, with at least one form of quenching processes.[3]

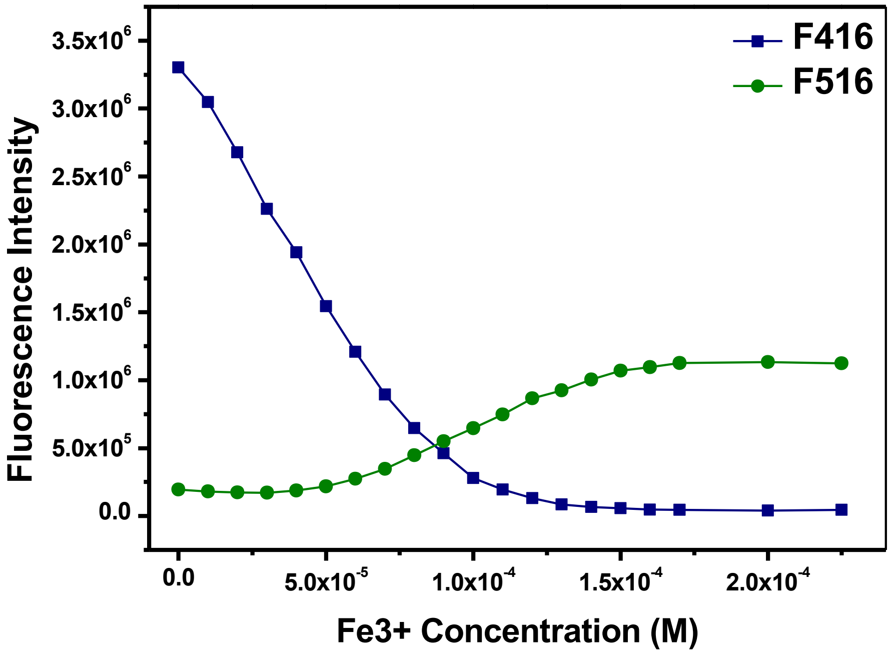

Fig. S5 Fluorescence intensity of BPVMB in ACN (50 μM) as a function of free Fe^{3+} at λ_{em}=416 nm (blue) and λ_{em}=516 nm (green). The disassociation constants (K_d) of BPVMB with Fe^{3+} in these two stages at 416 nm and 516 nm were calculated by equation 1 based on the emission spectroscopy to be 9.5×10^{-4} and 1.07×10^{-4}, respectively. The smaller dissociation constant for the second stage might indicates the BPVMB-Fe^{3+} complex formation at higher Fe^{3+} concentration.[4]

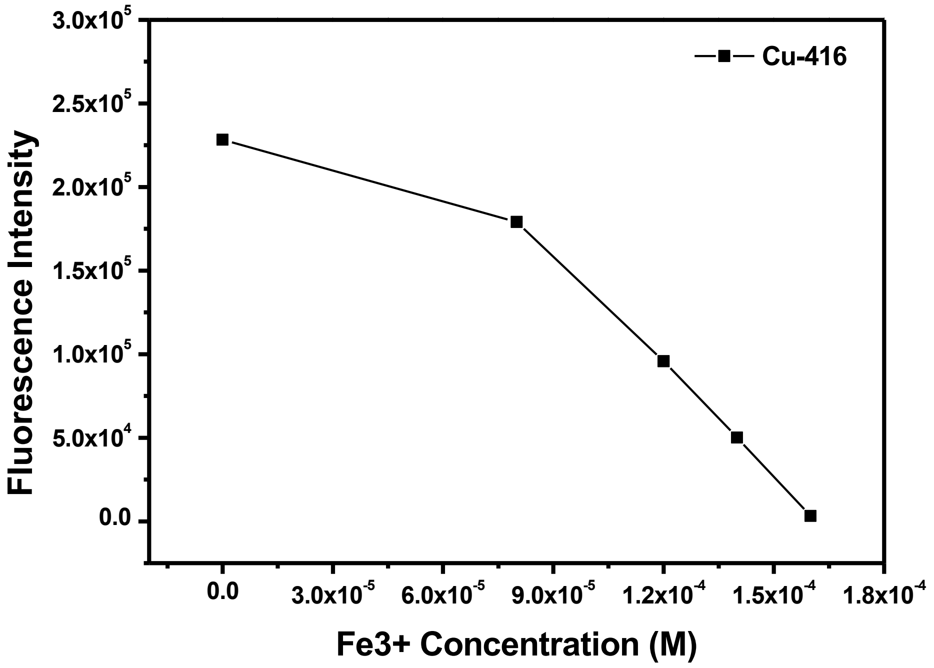

Fig. S6 Fluorescence intensity of BPVMB in ACN (50 μM) as a function of free Cu^{2+} at λ_{em}=416 nm. Fluorescence of BPVMB was quenched with addition of Cu^{2+}. The affinity (K_d) of BPVMB with Cu^{2+} was calculated by equation 2 to be 79.9× 10^{-4}.

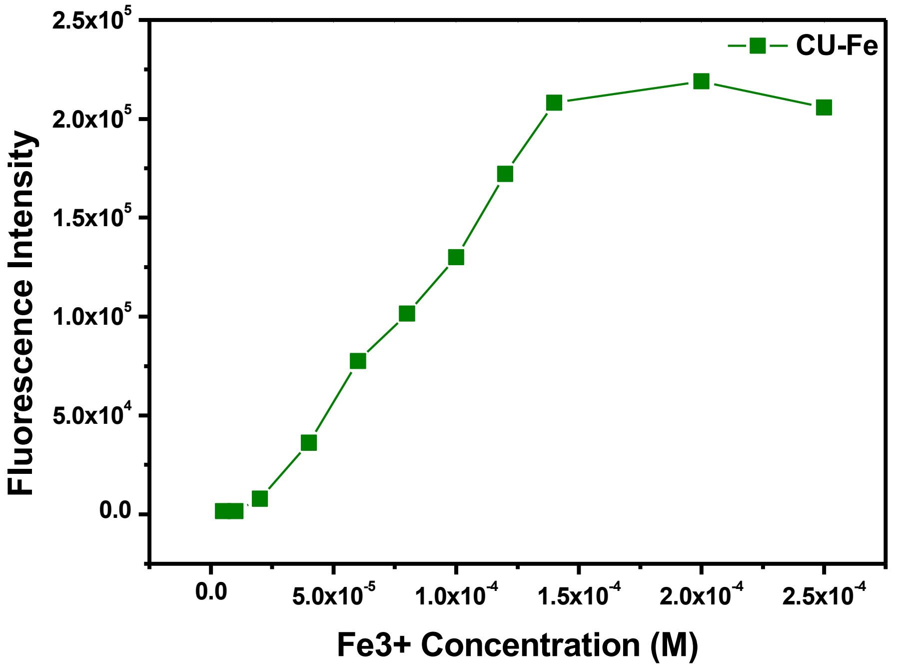

Fig. S7. Fluorescence intensity of BPVMB-Fe^{3+} in ACN (50 μM) as a function of free Fe^{3+} at λ_{em}=516nm. The affinity (K_d) of BPVMB with Fe^{3+} was determined by equation 1 to be 1.35× 10^{-4}, which was larger than that of BPVMB-Cu^{2+} (K_d=79.9× 10^{-4}). Therefore, when Fe^{3+} was added to the solution of BPVMB-Cu^{2+} complex, Cu^{2+} was displaced by Fe^{3+}.

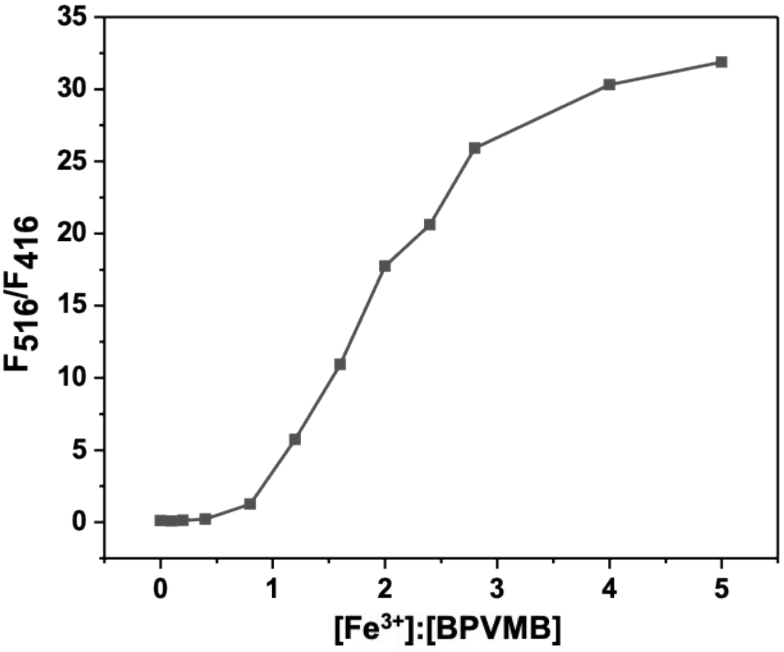

Fig. S8 The titration profile of BPVMB- Fe^{3+} in ACN (50 μM) based on the emission ratio at 516 and 416 nm, F_{516}/F_{416}. Excitation was at 320 nm. As can be seen, there is a linear dependence of the intensity ratios of emission at 516 nm to that of 416 nm (F_{516}/F_{416}) on when concentration of Fe^{3+}/ BPVMB is within the range from one to three, suggesting the addition of Fe^{3+} into the quenched BPVMB-Cu^{2+} complex leads to the emergence of green emission resulting from the formation of BPVMB-Fe^{3+}. The above results further validate that the non-fluorescent BPVMB -Cu^{2+} complex can be used as a latent off - on sensor for Fe^{3+}.

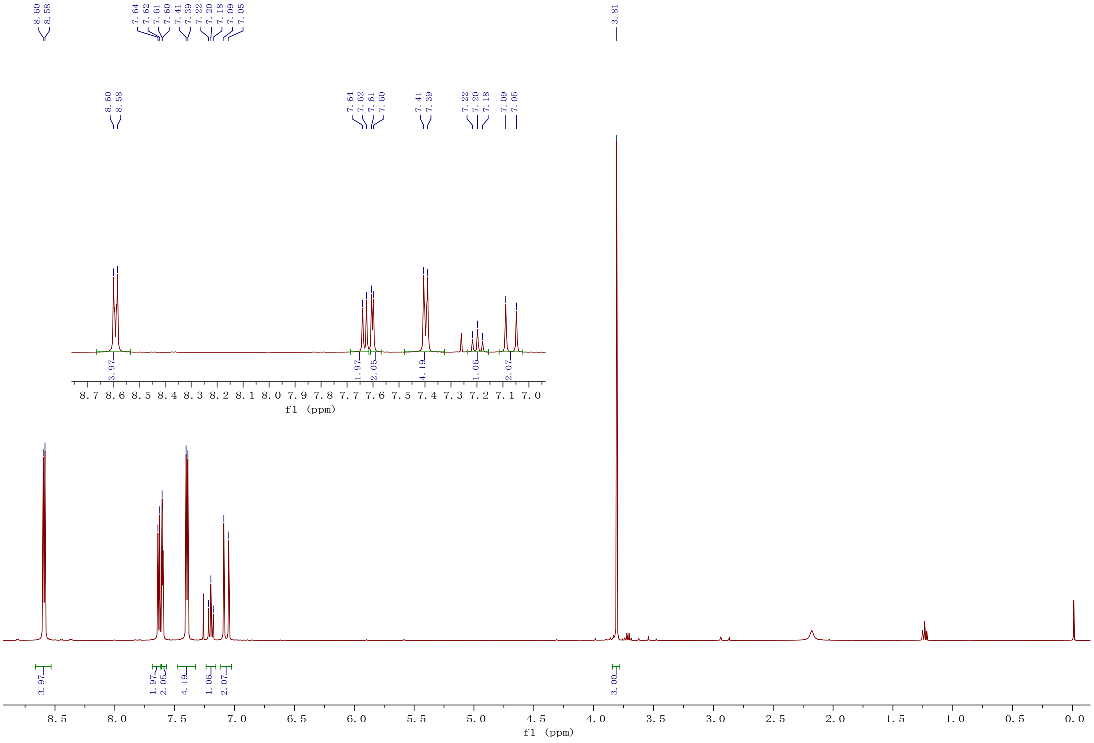

Fig. S9 ^{1}H-NMR spectrum of BPVMB

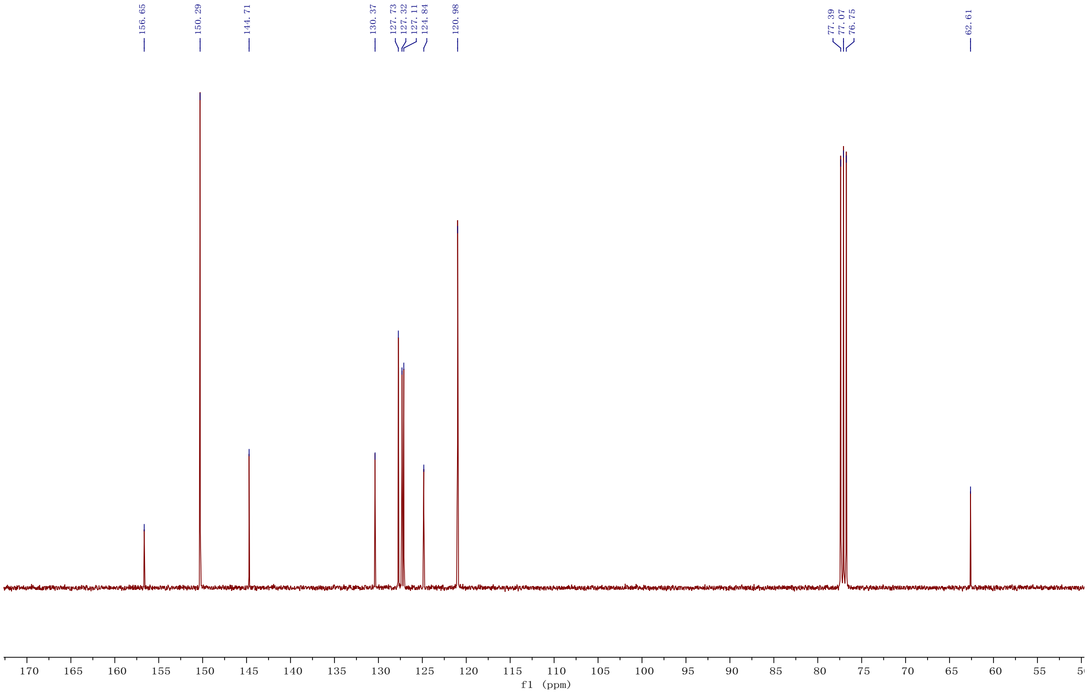

Fig. S10 ^{13}C-NMR spectrum of BPVMB

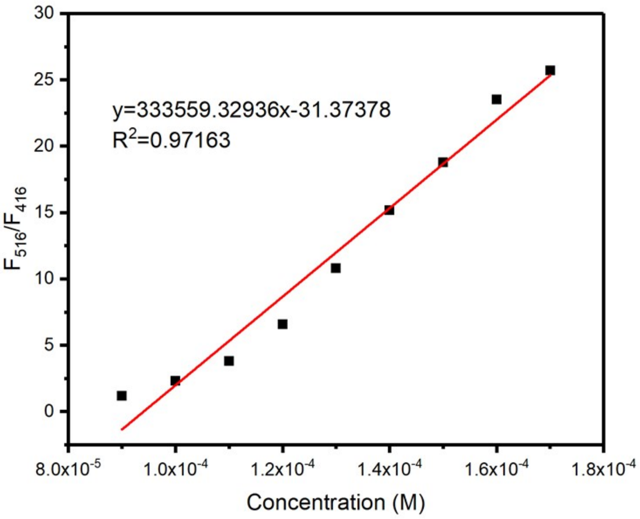

Fig. S11 Detection limit of BPMVB (50 µM) for Fe^{3+} based on emission ratio at 516 and 416 nm (F_{516}/F_{416}) by adding Fe^{3+} directly.

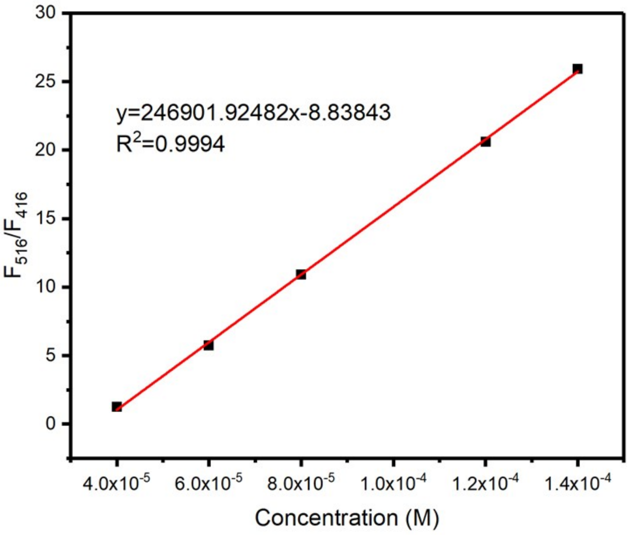

Fig. S12 Detection limit of BPMVB (50 µM) for Fe^{3+} based on emission ratio at 516 and 416 nm (F_{516}/F_{416}) by displacement approach.

Reference

1 Z. Xu, K.-H. Baek, H. Na Kim, J. Cui, X. Qian, D. R. Spring, I. Shin and J. Yoon, *J. Am. Chem. Soc.*, 2009, **132**, 601–610.

2 J. Cheng, X. Zhou and H. Xiang, *Analyst*, 2015, **140**, 7082–7115.

3 Z. Li, L. Zhang, L. Wang, Y. Guo, L. Cai, M. Yu and L. Wei, *Chem. Commun.*, 2011, **47**, 5798–5800.

4 V. K. Gupta, N. Mergu and L. K. Kumawat, *Sensors Actuators B Chem.*, 2016, **223**, 101–113.